Application of a Novel Analysis To Measure the Binding of the Membrane-Translocating Peptide Penetratin to Negatively Charged Liposomes†

Daniel Persson,*,‡ Per E. G. Thorén,‡ Mattias Herner, Per Lincoln, and Bengt Nordén

Department of Physical Chemistry, Chalmers University of Technology, SE-412 96 Gothenburg, Sweden

Received July 15, 2002; Revised Manuscript Received October 21, 2002

ABSTRACT: The binding of penetratin, a peptide that has been found useful for cellular delivery of large hydrophilic molecules, to negatively charged vesicles was investigated. The surface charge density of the vesicles was varied by mixing zwitterionic dioleoylphosphatidylcholine (DOPC) and negatively charged dioleoylphosphatidylglycerol (DOPG) at various molar ratios. The extent of membrane association was quantified from tryptophan emission spectra recorded during titration of peptide solution with liposomes. A singular value decomposition of the spectral data demonstrated unambiguously that two species, assigned as peptide free in solution and membrane-bound peptide, respectively, account for the spectral data of the titration series. Binding isotherms were then constructed by least-squares projection of the titration spectra on reference spectra of free and membrane-bound peptide. A model based on the Gouy−Chapman theory in combination with a two-state surface partition equilibrium, separating the electrostatic and the hydrophobic contributions to the binding free energy, was found to be in excellent agreement with the experimental data. Using this model, a surface partition constant of ∼80 M^{-1} was obtained for the nonelectrostatic contribution to the binding of penetratin irrespective of the fraction of negatively charged lipids in the membrane, indicating that the hydrophobic interactions are independent of the surface charge density. In accordance with this, circular dichroism measurements showed that the secondary structure of membrane-associated penetratin is independent of the DOPC/DOPG ratio. Experiments using vesicles with entrapped carboxyfluorescein showed that penetratin does not form membrane pores. Studies of the cationic peptide penetratin are complicated by extensive adsorption to surfaces of quartz and plastics. By modification of the quartz cell walls with the cationic polymer poly(ethylenimine), the peptide adsorption was reduced to a tolerable level. The data analysis method used for construction of the binding isotherms eliminated errors emanating from the remaining peptide adsorption, which otherwise would prevent a proper quantification of the binding.

Cellular uptake of polypeptides and oligonucleotides is generally poor, hampering the use of such molecules for, e.g., antisense applications. Recently, a novel approach for cytoplasmic delivery has been proposed on the basis of covalent linkage to a so-called cell-penetrating peptide (CPP[1]). CPPs are characterized by their ability to efficiently enter cells via a nonendocytotic and receptor- and transporter-independent pathway. Members of this class of compounds are, e.g., Tat-derived peptides, VP22, transportan, and penetratin (see refs *1* and *2* and references cited therein). Penetratin is a 16-residue fragment from the *Drosophila* transcription factor Antennapedia, corresponding to the third helix of the homeodomain. As for the other CPPs, the mechanism of membrane translocation is still obscure, but the results of cell studies (*3*−*5*) suggest that penetratin enters cells via direct interaction with membrane lipids. Hence, an understanding of the receptor-independent internalization process can be sought in studies of peptide−lipid interactions in model systems. The first reports in this area have dealt with the interactions of penetratin with liposomes (*6*−*10*), planar mono- and bilayers (*11*, *12*), and SDS micelles (*13*, *14*).

Since membrane association is the first step in all peptide−lipid interactions, characterization of the peptide binding is fundamental for the understanding of such processes. Generally, knowledge of the extent of binding is necessary for both the design of experiments and proper interpretation of the results. Binding isotherms can be constructed using a wide range of experimental techniques such as circular dichroism spectroscopy (*15*−*17*), isothermal titration calorimetry (*18*−*20*), monolayer area expansion (*21*, *22*), and fluorescence spectroscopy. In fluorescence binding studies, the fluorescence of intrinsic tryptophan residues in the peptide sequence (*23*, *24*) or that of a covalently linked fluorophore such as

† Supported by the Strategic Nucleic Acid Research Program and the Swedish Research Council.

* Corresponding author. Fax: (46)-31-7723858. E-mail: danielp@phc.chalmers.se.

‡ Both authors contributed equally to this work.

[1] Abbreviations: CD, circular dichroism; CPP, cell-penetrating peptide; DOPC, 1,2-dioleoyl-*sn*-glycero-3-phosphocholine; DOPG, 1,2-dioleoyl-*sn*-glycero-3-phosphoglycerol; DOPS, 1,2-dioleoyl-*sn*-glycero-3-phospho-L-serine; EDTA, ethylenediaminetetraacetic acid; Fmoc, 9-fluorenylmethoxycarbonyl; HEPES, *N*-(2-hydroxyethyl)piperazine-*N*′-2-ethanesulfonic acid; HPLC, high-performance liquid chromatography; LUVs, large unilamellar vesicles; NBD, 7-nitrobenz-2-oxa-1,3-diazol-4-yl; PEI, poly(ethylenimine); POPC, 1-palmitoyl-2-oleoyl-*sn*-glycero-3-phosphocholine; POPG, 1-palmitoyl-2-oleoyl-*sn*-glycero-3-phosphoglycerol; SDS, sodium dodecyl sulfate; SUVs, small unilamellar vesicles; SVD, singular value decomposition.

10.1021/bi026453t CCC: $25.00
Published on Web 12/10/2002

NBD (*25*, *26*) is utilized. In either case, one takes advantage of the shift in emission wavelength and increase in quantum yield that accompanies the transfer of the fluorophore from a polar environment (the aqueous solution) to a nonpolar environment (the lipid membrane). If possible, it is of course preferable to use the fluorescence of intrinsic tryptophan residues, since the chemical properties (such as the hydrophobicity) of the peptide are altered by the linkage to a fluorophore.

In this study, we have quantified the binding of penetratin to lipid vesicles by collecting tryptophan emission spectra at different peptide to lipid molar ratios. Quantitative studies of penetratin are complicated by extensive peptide adsorption to cuvette walls and the mixing device. The adsorption, which is of both electrostatic and hydrophobic nature, can be reduced to tolerable levels by modifying the surfaces of the cuvette with a cationic polymer, but titration spectra still does not show clean isosbestic points. However, by singular value decomposition of a matrix containing the acquired spectra, it is possible to establish that only two species, assigned as liposome-associated peptide and peptide free in solution, account for all spectral data. Least-squares projection of the titration spectra on reference spectra for peptide in solution and membrane-bound peptide is thus a proper data analysis that gives concentrations of free and bound peptide for the construction of binding isotherms. The membrane binding of penetratin is well described by a model based on the Gouy−Chapman theory in combination with a two-state partition equilibrium (*21*, *27*). In this approach, electrostatic and hydrophobic contributions to the membrane association of the peptide are treated separately, allowing an evaluation of the physical mechanism of binding. This makes it possible to compare the binding to membranes with various lipid compositions and to compare the binding properties of different peptides. The concentration of peptide at the membrane−water interface, several orders of magnitude higher than the bulk concentration due to the electrostatic attraction between the negatively charged vesicle membrane and the cationic peptide, is calculated using the Boltzmann equation. A surface partition equilibrium then relates the interfacial peptide concentration to the bound peptide to lipid ratio via the partition constant, K_p. For all lipid compositions used in this work, a good fit to experimental data is obtained by using a K_p of $\sim$80 M^{-1}, indicating that the hydrophobic contribution to the binding energy is independent of the fraction of negatively charged lipids in the membrane.

MATERIALS AND METHODS

Materials. 1,2-Dioleoyl-*sn*-glycero-3-phosphocholine (DOPC) was purchased from Larodan. 1,2-Dioleoyl-*sn*-glycero-3-phosphoglycerol (DOPG) and HEPES were obtained from Sigma. 1,2-Dioleoyl-*sn*-glycero-3-phospho-L-serine (DOPS) was purchased from Alexis Corp. EDTA (titriplex III) was purchased from Merck. Standard Fmoc-protected amino acids were obtained from Nova Biochem (Arg, Lys, Met, Trp, Phe), Alexis Corp. (Gln, Asn), and Perseptive Biosystems (Ile). [3-(Methylamino)propyl]trimethoxysilane and trimethylchlorosilane were from Fluka. 3-(Aminopropyl)triethoxysilane and poly(ethylenimine) [50% (w/v) aqueous solution] were purchased from Sigma. 5- (and 6-) carboxyfluorescein was obtained from Molecular Probes.

For circular dichroism measurements, a 5 mM sodium phosphate buffer (pH 7.4) was employed. For the induced leakage assay, the buffer used was 10 mM HEPES, 5 mM NaOH, 1 mM EDTA, and 107 mM NaCl (pH 7.4). The buffer used in all other experiments was 10 mM HEPES, 5 mM NaOH, 1 mM EDTA, and 0.1 M NaCl (pH 7.4). Deionized water from a Milli-Q system (Millipore) was used.

Peptide Synthesis. Penetratin (Arg-Gln-Ile-Lys-Ile-Trp-Phe-Gln-Asn-Arg-Arg-Met-Lys-Trp-Lys-Lys) was synthesized on a Pioneer peptide synthesizer (Perseptive Biosystems). Fmoc solid-phase synthesis was carried out on an Fmoc-PAL-PEG-PS support, resulting in an amidated carboxyl terminus after cleavage from the resin. After the synthesis was complete, the peptide was capped with an acetyl group at the amino terminus and cleaved from the resin with trifluoroacetic acid−1,2-ethanedithiol−water−triisopropylsilane (94:2.5:2.5:1). After precipitation by addition of cold ether, the peptide was collected by centrifugation, washed twice with ether, dried, dissolved in water, and lyophilized. Preparative reversed-phase HPLC (Kromasil C8 column, Eka Chemicals) was used to further purify the peptide (isocratic elution: water−2-propanol−trifluoroacetic acid volume ratios of 78/22/0.1). The identity of the peptide was confirmed by electrospray mass spectrometry.

Vesicle Preparation. Chloroform solutions of DOPC and DOPG were mixed to obtain the desired ratio of zwitterionic and negatively charged lipids, and the solvent was removed with a rotary evaporator. The dry phospholipid film was placed in high vacuum for 2 h to remove trace amounts of chloroform. Vesicles for binding studies and circular dichroism mesasurements were prepared by dispersion of the lipid film in buffer. Vesicles with encapsulated carboxyfluorescein for leakage experiments were prepared by dispersion of the lipid film in a 10 mM HEPES, 50 mM carboxyfluorescein, 10 mM NaCl, 148 mM NaOH, and 1 mM EDTA (pH 7.4) solution. The dispersion was subjected to five freeze−thaw cycles (*28*) before extrusion 21 times through two 100 nm polycarbonate filters on a LiposoFast-Pneumatic extruder (Avestin, Canada) to obtain large unilamellar vesicles (LUVs). The lipid concentration was determined by the Stewart assay (*29*). A homogeneous liposome size distribution around 100 nm was confirmed by dynamic light scattering analysis, using a Malvern Instrument Series 7032 Multi-8 correlator and a PCS100 spectrometer (Malvern Instruments).

Binding Experiments. Fluorescence experiments were performed on a Spex Fluorolog τ-3 spectrofluorometer (JY Horiba) using a 1 $\times$ 1 cm quartz cell thermostated at 25.0 °C. The band-pass of the excitation slit was set to 0.7 nm in order to obtain an optimal signal to noise ratio without photodegradation. Spectra were recorded between 315 and 400 nm with an increment of 1 nm and an integration time of 2 s. The total concentration of peptide in the samples ranged from 0.5 to 3 μM. Peptide solution was titrated with microliter aliquots of liposome stock solution (5 or 10 mM), and a spectrum was acquired after every vesicle addition. Penetratin has earlier been shown to induce vesicle aggregation followed by spontaneous disaggregation, resulting in restitution of the initial, nonaggregated liposome population (*7*). The presence of large aggregates is expected to influence the absorption as well as the fluorescence of the sample, thereby distorting the apparent binding isotherms. Therefore,

the samples were checked for aggregation by static light scattering with both the excitation and the emission monochromators set to 600 nm. In a few cases, the first liposome addition, leading to high peptide to lipid molar ratios, resulted in minor aggregation. The spectrum was then recorded after the subsequent disaggregation. The tryptophan spectra acquired during the following titration overlapped with those obtained in a control experiment, in which the titration did not involve any aggregation (a larger amount of liposomes was added initially). This justifies the conclusion that the liposomes are indeed intact during the entire aggregation−disaggregation process. Also, performing the titrations in the reversed order, i.e., titrating a liposome solution with aliquots of penetratin stock solution, resulted in the same binding isotherms (data not shown).

Mixing of the cuvette contents was achieved by plunging a cuvette mixer three times up and down. It was shown in separate experiments using various fluorophores that this procedure was sufficient for complete mixing. The cuvette mixer was constructed in stainless steel with a straight handle and a rhombic footprint with diagonals of 13 and 10 mm.

The surface of the interior cuvette walls was modified by leaving the cuvette filled with a 1% (w/v) solution of poly(ethylenimine) in deionized water at room temperature for 30 min. The cell was then rinsed thoroughly with deionized water.

Adsorption Experiments. Peptide adsorption was quantified by continuously measuring the emission at 350 nm with excitation at 290 nm. The cuvette was carefully filled with premixed peptide solution, and the fluorescence intensity was recorded for 5 min before stirring was initiated. A Spinfin magnetic stirring bar with Teflon coating (Bel-Art Products, Pequannoc, NJ) was used.

Analysis of Binding Data. Spectra were corrected by subtracting the vesicle background, measured in a separate experiment, and analyzed using Matlab (The MathWorks Inc.). For singular value decomposition of the titration spectra (eq 1, vide infra), the Matlab command *svd* was employed, and for least-squares projection of titration spectra on reference spectra (eq 3), the *pinv* command was used.

Circular Dichroism Measurements. Circular dichroism (CD) was measured on a Jasco J-810 spectropolarimeter using a 1 mm quartz cell. All spectra were taken between 190 and 260 nm and corrected for background contributions. Results are expressed as mean residue ellipticities $[\theta]_{MR}$ (deg cm^2/dmol). Reference CD spectra were taken from Perczel et al. (*30*). Secondary structure evaluation was performed by least-squares projection of the acquired spectra (between 195 and 240 nm) on α-helix, antiparallel β-pleated sheet, and random coil reference spectra using Matlab.

Induced Leakage Assay. The efflux experiments were performed at 25 °C on a Spex Fluorolog τ-3 spectrofluorometer (JY Horiba). The nonentrapped dye was separated from the vesicles on a Sephadex G-50 column (Amersham Pharmacia Biotech) by using an isoosmolar buffer (see above). Lipid concentrations were determined by static light scattering at 600 nm, using a standard curve. Peptide-induced leakage of vesicle-entrapped carboxyfluorescein was monitored using excitation and emission wavelengths of 490 and 520 nm, respectively. The liposomes were diluted with buffer in a 1 × 1 cm quartz cell before addition of peptide. Starting with a self-quenching concentration of carboxyfluorescein inside the liposomes, any leakage of the dye can be detected as an increase in the fluorescence intensity. The peptide-induced leakage can be quantified by relating it to the effect of lysing the vesicles with Triton X-100. The self-leakage of the dye was found to be negligible and was not affected by the PEI modification of the cuvette walls.

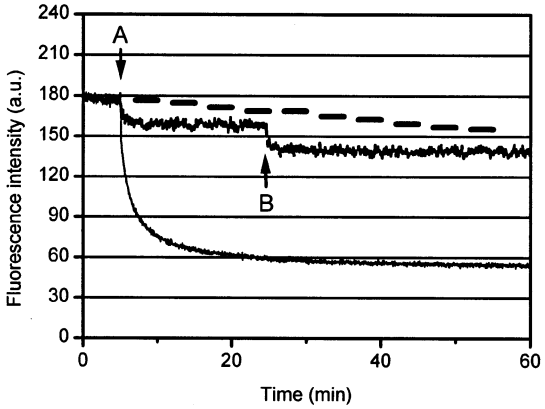

FIGURE 1: Penetratin adsorption upon stirring a 0.5 μM solution in a 1 × 1 cm quartz cell monitored using tryptophan emission at 350 nm. Arrow A indicates initiation of stirring. (Lower trace) Ordinary quartz cell with a Teflon magnetic stirring bar. (Upper trace) Poly(ethylenimine)-modified quartz cell with a Teflon magnetic stirring bar. Arrow B indicates initiation of stirring after replacing the stirring bar with a new one. (Horizontal bars) Poly(ethylenimine)-modified quartz cell where mixing is accomplished using a stainless steel cuvette mixer (described in Materials and Methods). The mixer is plunged through the sample solution three times every 5 min. Each such mixing event is enough to achieve complete mixing. For clarity, bars are used to represent the time average of the fluorescence intensity recorded between mixing events.

RESULTS AND DISCUSSION

Peptide Adsorption. As will be inferred, earlier studies of the binding of penetratin to vesicles have most likely been prone to artifacts due to adsorption of peptide during the experiments. The adsorption is extensive due to both electrostatic and hydrophobic types of interaction and not easily avoided. Therefore, we will devote the first section to this important problem and how it can be solved.

When stirring a 0.5 μM penetratin solution in a 1 × 1 cm quartz cell with a Teflon magnetic stirring bar, about 70% of the peptide fluorescence is lost before a stable level is reached (Figure 1, lower trace). That this is due to adsorption of peptide molecules to the walls of the cuvette and to the stirring bar is demonstrated by a number of supplementary experiments. First, the rapid decrease in fluorescence is intimately related to stirring since when the unstirred solution is monitored, the decay is very slow. Corresponding observations are made when measuring absorbance. Mixing of the cuvette contents with a pipet also results in a substantial loss of signal. Second, the fluorescence decrease does not depend on exposure to light. Third, if the cuvette contents are transferred to a new cuvette, after the signal has decayed to a constant level, a similar fluorescence decrease is obtained upon stirring. Fourth, replacing the stirring bar with a new one, after the signal has decayed to a constant level, also results in another rapid reduction of the fluorescence. These observations exclude that the apparent decrease in peptide concentration is due to photodegradation or to peptide

aggregation in solution, the latter giving diminution of fluorescence due to self-quenching or to absorption statistics.

Penetratin, formally carrying seven positive charges, has a propensity to adhere to the electronegative surface of quartz (fused silica) cells. No systematic study of the adsorption of cationic peptides has been reported before, but similar problems due to cuvette adsorption have been noticed for magainin (*31*) and melittin (*32*). In the case of penetratin, we have observed considerable adsorption also to the surfaces of plastic materials such as Teflon magnetic stirring bars (see above), standard polypropylene pipet tips, and cuvettes made of polystyrene and poly(methyl methacrylate) (data not shown). Adhesion of cationic peptides to surfaces is governed by contributions from both electrostatic and hydrophobic interactions, the main constituent of the latter being the entropic gain associated with dehydration of the peptide molecules and the surface (*33*). For the interaction of penetratin with negatively charged surfaces such as that of quartz, the electrostatic contribution probably dominates. However, the hydrophobic influence might be significant, considering the extensive adsorption to nonpolar plastic surfaces.

Peptide adsorption of course leads to uncertainties as to the actual concentration in the sample. This severely complicates quantitative experiments, especially since peptide may later be desorbed from surfaces as the conditions in the solution are changed, e.g., by addition of liposomes (data not shown). To reduce the problems associated with peptide adhesion to quartz cuvettes, modification of the surface is necessary. However, standard methods such as silanization using, e.g., [3-(methylamino)propyl]trimethoxysilane, 3-(aminopropyl)triethoxysilane, and trimethylchlorosilane only resulted in marginal improvements. Instead, the effect of surface-bound poly(ethylenimine) (PEI) was investigated. The strong electrostatic interaction between this cationic polymer and the negatively charged silica surface makes modification very simple. The polymer is simply adsorbed to the surface from an aqueous solution, the adsorption being virtually irreversible (*34*). PEI proved to be very effective in preventing penetratin adsorption. In Figure 1 (middle trace), the result of stirring a penetratin solution in a PEI-modified cuvette using a Teflon magnetic stirring bar is shown. Compared to the analogous experiment using an ordinary quartz cell (lower trace), the decrease is quite small (10−15%). The loss of peptide that still occurs can almost exclusively be ascribed to the Teflon stirring bar, as replacing the stirring bar with a new one results in a renewed, equally large peptide loss (see Figure 1, arrow B). The peptide adsorption to the stirring bar and the fact that liposome addition leads to partial desorption necessitate employment of a different mixing technique. When a stainless steel cuvette mixer (described in Materials and Methods) is used, a comparatively small loss of peptide (∼1%, upper trace) is observed at each mixing event. Therefore, this approach is recommended, especially for experiments where the sample needs to be mixed only once, as in the measurement of reference spectra of free and membrane-bound peptide (see below).

Binding Isotherms. The blue shift in the fluorescence emission maximum and the change in quantum yield observed when tryptophan is transferred from a polar medium to a less polar environment can be utilized to study the binding of peptides to lipid membranes. Figure 2A shows a typical example of the influence of stepwise liposome addition on the tryptophan emission spectrum of penetratin. In aqueous buffer, the emission has its maximum at 350 nm, indicating that the tryptophan residues are fully exposed to the water solvent. Introduction of liposomes in the solution causes the peptide molecules to equilibrate between the lipid membranes and the solvent, leading to a shift of the tryptophan fluorescence maximum and an increase in fluorescence intensity. At a certain lipid concentration, no further change in the spectrum is observed after background correction, corresponding to a final state where all the peptide is associated with the liposomes. The membrane-bound peptide exhibits a fluorescence maximum around 337 nm.

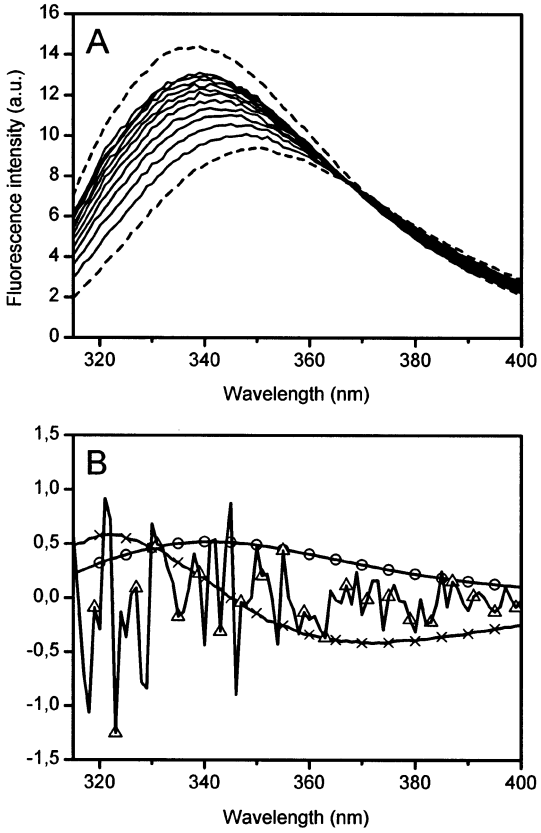

FIGURE 2: (A) Tryptophan emission spectra aquired when titrating peptide with liposome stock solution. Dashed curves indicate reference spectra of peptide free in solution (lower trace) and membrane-bound peptide (upper trace) collected in separate experiments. (B) The first three columns of *U* from the singular value decomposition of the titration spectra in (A). While the first two components (○ and ×) are sufficient to describe the data, the third (△) only contains noise. Relative singular values: 0.9164, 0.0661, and 0.0018.

When constructing the binding isotherms from fluorescence data, the intensity at a fixed wavelength is frequently used to estimate the extent of binding. The simplest approach for evaluating the collected data is to assume that only two states exist: peptide free in solution and membrane-associated peptide (*35*−*37*). If this is the case, the fluorescence intensity increases with the lipid concentration and asymptotically approaches a final value as the lipid to peptide molar ratio is increased. On the basis of the initial and the final signals, the amount of free and bound peptide can easily be obtained. However, when the fluorescence intensity at 337 nm was used to monitor the membrane binding of penetratin,

the signal decayed at the end of the titration, i.e., at high lipid concentrations. Such a decrease is often attributed to light scattering effects (*24*, *38*). We therefore investigated the influence of light scattering on our fluorescence measurements by titrating micromolar concentrations of free tryptophan with liposomes. That the free amino acid at these concentrations does not significantly interact with the liposomes was evidenced by a lack of blue shift upon titration (data not shown). Thus, any attenuation of the signal can be ascribed to the increase in turbidity associated with the addition of liposomes. We found that the tryptophan fluorescence decreased almost linearly with lipid concentration up to 1.5 mM, where the fraction of scattered light was 13% (data not shown). In the concentration range used in this work, however, the decrease is much less (<2%). Correction of the collected data from the peptide binding measurements using this result had only a minor effect on the outcome. An alternative possibility is that the decrease in peptide fluorescence stems from the coexistence of several membrane-bound states with different spectral properties. One approach found in the literature allows for variation of the fluorescence intensity of the membrane-bound peptide with the concentration of peptide in the membrane (*23*, *39*, *40*). However, we find that, at least in the case of penetratin, the main cause of reduction of tryptophan fluorescence is a concentration decrease due to adsorption of peptide to the cuvette walls, pipet tips, and the mixing device during the titration (see above). This precludes a correct evaluation of binding data from the fluorescence signal at a fixed wavelength.

A more adequate method of analysis is to collect the entire tryptophan emission spectrum at each point of the titration and to project these spectra on membrane-bound and free peptide reference spectra, as proposed by Polozov et al. (*41*). We find this procedure suitable here, especially when considering the problems with decreasing total peptide concentration during the titration. The reference spectra for peptide in solution and peptide associated with liposomes can be obtained in separate experiments, where the samples are mixed only once, minimizing peptide adsorption.

For calculation of the binding isotherms of penetratin, a procedure involving least-squares projection in combination with singular value decomposition (SVD) was used (*42*) (see also Materials and Methods). The spectra were collected as columns with one intensity value per wavelength in a matrix of data *D*. This matrix was factorized by SVD according to

$$D = USV^T \tag{1}$$

where *U* and *V* have orthonormal columns ($U^TU = V^TV = I$) and *S* is zero except along the diagonal which contains the nonnegative *singular values*. It was found that only two singular values were significantly larger than zero and that they were the only singular values associated with nonrandom *U* columns (see Figure 2B). This is consistent with the hypothesis that two species, free and bound peptide, within experimental errors, account for the emission spectra of the whole titration:

$$D \approx RC^T \tag{2}$$

where *R* is the reference spectra matrix and *C* is the peptide concentration matrix. *R* thus has two columns, the emission spectra of free and bound peptide at unit concentration, respectively, and the two columns of *C* contain the concentrations of free and membrane-bound peptide, C_f and C_b, in the titration. The concentrations *C* could be obtained by a least-squares projection of the emission spectra in *D* on the space of *R*:

$$C^T = (R^TR)^{-1}R^TD \tag{3}$$

To ensure a negligible concentration of free peptide when measuring the reference spectrum of bound peptide, an excess lipid concentration was used, corresponding to 150% of that of the point in the titration where no further blue shift was observed. However, when using liposomes with only 10% DOPG, the surface charge density is low and the peptide binding relatively weak. Therefore, the reference spectrum of membrane-bound peptide was in this case not measured by simply adding an excess of lipid, since the required amount of liposomes would lead to complications due to light scattering. Instead, the bound reference spectrum was calculated from the free reference spectrum and a spectrum where most of the peptide was bound. The fraction of free peptide in the latter (~9%) was estimated by assuming that the emission maximum wavelength of the bound peptide matches that obtained for the other lipid compositions (~337 nm). When the resulting C_f and C_b values were applied in the binding model (see below), an excellent fit to the experimental data was obtained. Also, the data point with an estimated fraction of free peptide coincided with the calculated binding curve, justifying the assumption.

With C_f and C_b determined for every lipid concentration, *L*, in the titration, the membrane-bound peptide to lipid molar ratio

$$r = C_b/L \tag{4}$$

can be calculated, allowing construction of the binding isotherm, *r* versus C_f. Figure 3A shows the binding isotherms of penetratin for a number of DOPC/DOPG molar ratios. There is a marked curvature, reflecting the decreased electrostatic attraction between the peptide and the membrane as more and more peptide becomes associated with the liposomes. This is well-known for peptides carrying a net charge, e.g., melittin (*15*). In calculating *r*, the peptide was assumed to have access to both leaflets of the vesicle membranes as it has previously been shown to be able to translocate across a pure lipid bilayer (*6*). As expected, the membrane affinity of the cationic peptide is highly dependent on the fraction of negatively charged lipids. As a first approximation, the apparent binding constant

$$K_{app} = r/C_f \tag{5}$$

is calculated from the initial slope of the binding isotherm. K_{app} increases markedly with the DOPG content (see Table 2), reflecting the importance of the electrostatic interactions. The value obtained for DOPC/DOPG (70/30) (4.5×10^6 M^{-1}) is considerably higher than that reported by Drin et al. (*9*) for POPC/POPG (70/30) (1.3×10^4 M^{-1}, referred to as "K_p"). In an extension of that study (*10*), using an NBD-labeled penetratin, the apparent binding constant was found to be ~2.2×10^5 M^{-1} for POPC/POPG (75/25), suggesting a strong influence of the NBD fluorophore on the membrane

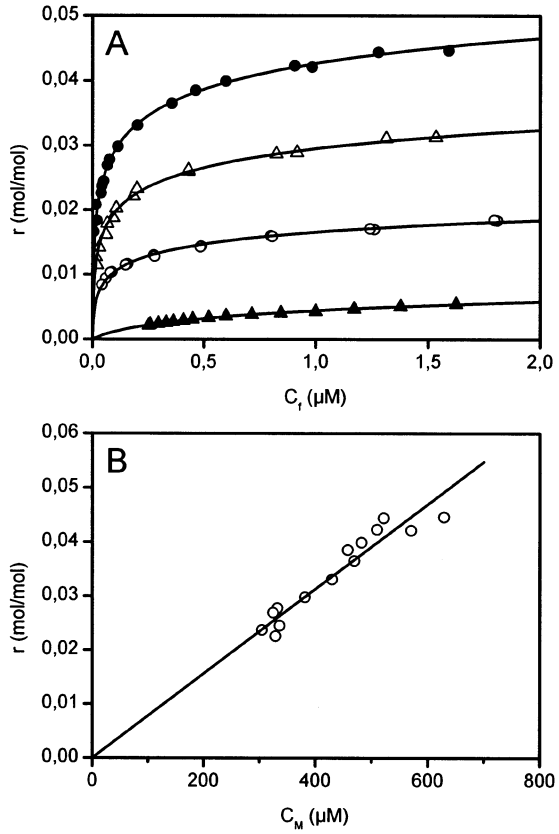

FIGURE 3: (A) Binding isotherms for the association of penetratin to vesicles with DOPC/DOPG molar ratios of (●) 60/40, (△) 70/30, (○) 80/20, and (▲) 90/10. The membrane-bound peptide to lipid molar ratio, r, is plotted against the free peptide concentration in bulk solution, C_f. The solid lines correspond to theoretical binding isotherms calculated according to a model combining the Gouy−Chapman theory with a surface partition equilibrium (see text for details). Values of the effective peptide charge, z_p, and the surface partition constant, K_p, are given in Table 2. (B) The membrane-bound peptide to lipid molar ratio, r, is plotted against the calculated peptide concentration immediately above the membrane surface, C_M, for DOPC/DOPG (60/40). C_M is much higher than C_f, reflecting the strong electrostatic attraction between the peptide and the membrane. The surface partition constant, theoretically free from electrostatic contribution, is given by the slope of the linear fit.

affinity of the peptide. In both cases, however, there are no comments on peptide adsorption despite the use of constant stirring with a magnetic stirring bar. The shapes of the binding isotherms differ significantly from ours. For instance, the experimental binding isotherms of ref *10* do not point toward the origin, presenting a physically unrealistic picture.

Binding Model Separating Electrostatic and Hydrophobic Contributions. Since electrostatic interactions are not considered, describing the binding of charged peptides in terms of a simple partition equilibrium or a Langmuir adsorption isotherm does not allow an evaluation of the physical mechanism of binding. Instead, the electrostatic and hydrophobic contributions to the membrane affinity of the peptide need to be dealt with separately. The analysis presented here follows the approach proposed by Beschiaschvili and Seelig (*21*) for binding of cationic peptides to neutral and negatively charged lipids. This model is based on the Gouy−Chapman theory and has been employed to describe the membrane association of a number of peptides (*19*, *20*, *22*, *43*).

The surface charge density, σ, of the DOPC/DOPG membranes is given by

$$\sigma = (e_0/A_L)\frac{-X_{PG}(1 - X_{Na}) + z_p r}{1 + (A_P/A_L)r} \quad (6)$$

where e_0 is the elementary charge, A_L the area per lipid molecule, A_P the effective area of the peptide in the membrane, z_p the effective charge of the peptide, and X_{PG} the mole fraction of DOPG in the membrane. A_L was assumed to be equal for DOPC and DOPG headgroups and was set to 70 Å^2. The actual value of A_P for penetratin has never been measured experimentally. The value used here (150 Å^2) is similar to that used for other peptides (*16*, *21*, *22*) but must be considered rather arbitrarily chosen, since the extent of penetratin insertion into the membrane is unknown. However, since r never exceeds 0.045 in our experiments, the contribution from the correction term for peptide insertion, $(A_P/A_L)r$, is small compared to unity. The choice of A_P is thus not critical for the calculations. The reduction of the surface charge density due to counterion binding is accounted for by including X_{Na}, which denotes the mole fraction of DOPG associated with Na^+. It is calculated by assuming a Langmuir adsorption isotherm

$$X_{Na} = \frac{K_{Na}C_{M,Na}}{1 + K_{Na}C_{M,Na}} \quad (7)$$

where K_{Na} is the Na^+ binding constant, taken as 0.6 M^{-1} (*44*) and $C_{M,Na}$ is the concentration of sodium ions in the close proximity of the membrane surface. $C_{M,Na}$ is connected to the bulk equilibrium concentration, $C_{eq,Na}$, and the surface potential, ψ_0, via a Boltzmann distribution

$$C_{M,Na} = C_{eq,Na}\exp(-\psi_0 F/RT) \quad (8)$$

where F is the Faraday constant, R the gas constant, and T the absolute temperature.

The surface potential can be determined by combining eq 6 with the Gouy−Chapman equation

$$\sigma^2 = 2000\epsilon_0\epsilon_r RT\sum_i C_{i,eq}(e^{-z_i F_0\psi_0/RT} - 1) \quad (9)$$

where ϵ_0 is the permittivity in a vacuum, ϵ_r denotes the relative dielectric permittivity of water, $C_{i,eq}$ is the bulk concentration of the ith electrolyte, and z_i is its signed valency. The peptide concentration immediately above the membrane surface, C_M, is given by

$$C_M = C_f\exp(-z_p F\psi_0/RT) \quad (10)$$

Having thus accounted for the electrostatic interaction between the peptide and the membrane, the binding can be described by a surface partition equilibrium

$$r = K_p C_M \quad (11)$$

where K_p is the surface partition constant.

For a range of z_p values, eqs 6−10 were solved for each experimental value of r and C_f. The resulting C_M values were plotted against r in search of the z_p that corresponds to the best fit to the experimental data according to eq 11. A representative example is given in Figure 3B, which shows

Table 1: Experimental Data and Calculated Parameters (with $z_p = 4.9$) for Penetratin Binding to DOPC/DOPG (60/40) Liposomes

C_f (μM)[a]	r (mol/mol)[b]	σ (mCi/m^2)[c]	ψ_0 (mV)[d]	C_M (μM)[e]
0.039	0.0226	−39.1	−47.3	322.5
0.041	0.0237	−38.4	−46.6	298.5
0.050	0.0245	−37.8	−46.1	329.1
0.066	0.0269	−36.1	−44.4	317.6
0.076	0.0278	−35.5	−43.8	324.7
0.114	0.0298	−34.1	−42.4	372.9
0.202	0.0331	−31.9	−40.0	419.2
0.355	0.0365	−29.5	−37.5	456.8
0.463	0.0385	−28.1	−36.0	445.2
0.598	0.0399	−27.1	−34.9	468.4
0.907	0.0423	−25.5	−33.0	495.0
0.984	0.0421	−25.6	−33.2	553.9
1.280	0.0444	−24.0	−31.3	506.0
1.592	0.0446	−23.9	−31.2	610.4

[a] Free peptide concentration in bulk solution. [b] Membrane-bound peptide to lipid molar ratio. [c] Membrane surface charge density. [d] Membrane surface potential. [e] Concentration of peptide immediately above the membrane surface.

Table 2: Summary of Binding Parameters

DOPC/DOPG (mol/mol)[a]	K_p (M^{-1})[b]	z_p[c]	K_{app} (M^{-1})[d]
60/40	81	4.9	9.2×10^6
70/30	95	5.1	4.5×10^6
80/20	89	5.8	1.5×10^6
90/10	67	5.5	1.6×10^4

[a] DOPC to DOPG molar ratio. [b] Surface partition constant. [c] Effective peptide charge. [d] Apparent binding constant.

the linear relationship between r and C_M for DOPC/DOPG (60/40) using a z_p of 4.9. The corresponding set of calculated parameters is summarized in Table 1. C_M is obviously much higher than C_f, reflecting the strong electrostatic attraction between the membrane with its negative surface potential and the positively charged peptide. As expected, the surface potential and the surface charge density decrease in magnitude due to partial neutralization of the DOPG headgroups as peptide is associated with the membrane. This, in turn, lowers the affinity of the peptide for the liposomes, which accounts for the curvature of the conventional binding isotherms.

The calculated binding isotherms are in excellent agreement with the experimental data and are included as solid curves in Figure 3A. In Table 2, the optimal values of z_p and the corresponding values of K_p for the different lipid compositions are summarized. The calculated z_p values are smaller than the formal charge, which is +7 (both the carboxyl terminus and the amino terminus are end capped). This observation has been made in studies of a number of charged peptides and has been attributed mainly to discrete charge effects (see refs *15* and *45* and references cited therein), separation of charges in the peptide (*46*, *47*), and effects of associated counterions (*15*). The values of the partition constant (K_p) fall in a narrow range, indicating that the hydrophobic contribution to the binding energy is a general feature, virtually independent of the content of acidic lipids. This indicates that penetratin is drawn to the membrane by nonspecific electrostatic attraction and does not bind specifically to any of the lipids used. We found further support for this conclusion when using another acidic lipid, DOPS, instead of DOPG. For DOPC/DOPS (60/40), a binding isotherm (data not shown) very similar to that of the corresponding DOPC/DOPG ratio and with an equally good fit to the calculated binding isotherm was obtained ($z_p = 4.6$ and $K_p = 99$ M^{-1}). Interestingly, however, in the titrations using liposomes containing DOPS, the blue shift of the tryptophan fluorescence upon binding was accompanied by a small decrease in quantum yield (~10%). We do not yet know the origin of this intensity change, but it is possible that the presence of the dipolar serine headgroup may somewhat change the energies of the La and Lb states of the indole chromophore, thereby changing the transition probabilities. Whatever the origin of the decrease in fluorescence intensity, singular value decomposition of the titration spectra showed that two species account for the spectral data just as in the case of DOPC/DOPG liposomes, justifying the use of our method of analysis based on reference spectra of free and bound peptide.

The K_p of penetratin presented in this work (~80 M^{-1}) is comparable to what has been found for other moderately hydrophobic peptides such as magainin 2 amide ($K_p = 50$ M^{-1}) (*19*) and SMS 201−995 ($K_p = 70$ M^{-1}) (*43*) but considerably lower than for melittin ($K_p = 4.5 \times 10^4$ M^{-1}) (*16*) with its high content of nonpolar amino acids.

For all lipid compositions, the surface partition constant, K_p, and the apparent binding constant, K_{app}, differ by several orders of magnitude. The total free energy of binding can be calulated as

$$\Delta G = -RT\left[\ln 55.5 + \ln K_p + \ln\left(\frac{C_M}{C_f}\right)\right] \qquad (12)$$

where the term ln 55.5 provides the cratic contribution (*48*), which amounts to −2.4 kcal/mol, the term ln K_p provides the hydrophobic contribution to the binding energy (*20*, *22*), and ln(C_M/C_f) provides the electrostatic contribution and equals ln(K_{app}/K_p), when evaluated at a low degree of binding. By insertion of the binding constants for DOPC/DOPG (60/40) (see Table 2), the hydrophobic and electrostatic free energy contributions are found to be −2.6 kcal/mol and −6.9 kcal/mol, respectively. The electrostatic part thus dominates, but even for the membranes containing a large fraction of acidic lipids, the hydrophobic contribution is significant. The main driving forces for the partitioning of peptide into the membrane are the so-called hydrophobic effect (the energy gain of removing the nonpolar parts of the peptide from the aqueous phase) (*49*) and the formation of inter- or intramolecular hydrogen bonds as the peptide forms a secondary structure (*50*). For comparison with our experimentally determined hydrophobic free energy, we calculated both the free energy for partitioning of the unfolded peptide into the membrane interface using the whole residue hydrophobicity scale of Wimley and White (*51*) and the free energy of folding on the basis of the results of studies of the energetics of helix formation using melittin (*50*). For the penetratin sequence, the free energy of partitioning was found to be +0.5 kcal/mol, taking into account the amidation of the C-terminus (*52*). With a helical content of 60% (from CD measurements; see below), one can estimate the folding free energy of penetratin to be −3.9 kcal/mol. The sum of these contributions equals −3.4 kcal/mol, which is relatively close to our experimental value, −2.6 kcal/mol. Furthermore, for a peptide with a hydrophobic free energy of −3.4 kcal/mol

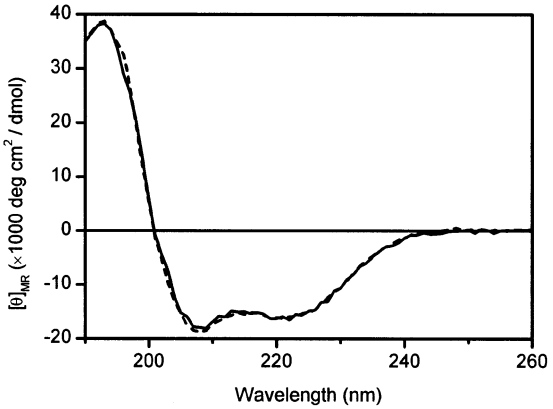

FIGURE 4: Circular dichroism spectra of penetratin bound to liposomes with DOPC/DOPG molar ratios of 60/40 (dashed line) and 80/20 (solid line). The peptide concentrations used in these experiments were 8 and 6 μM, and the concentrations of lipid were 400 and 800 μM, respectively. The fact that the two spectra are essentially identical and coincide with that of penetratin bound to DOPG vesicles (data not shown) indicates that the conformation of membrane-bound penetratin is independent of the DOPC/DOPG ratio. All spectra were recorded at peptide to lipid molar ratios where no vesicle aggregation occurs.

and a formal charge of +7, a recently proposed empirical rule of thumb (*53*) predicts an effective peptide charge of +5.4, which falls within the range of z_p values reported in Table 2.

Peptide Conformation. The conformation of penetratin in various membrane-mimicking model systems has been the subject of a number of studies. We have earlier reported that penetratin adopts an α-helical conformation upon binding to DOPG LUVs (*7*) at low peptide to lipid molar ratios. α-Helix formation of penetratin has also been observed at low peptide to lipid ratios for POPC/POPG (70/30) SUVs (*9*, *54*) and POPG SUVs (*54*). In SDS micelles, the peptide is also present in an α-helical conformation (*9*, *13*, *14*). On the other hand, at elevated peptide to lipid ratios, we have observed formation of antiparallel β-pleated sheets in DOPG LUVs, the transition from an α-helical to a β-sheet conformation being strongly coupled to vesicle aggregation (*7*). Penetratin has also been shown to adopt a β-sheet conformation when associated with a DPPC/DPPS monolayer at the air/water interface (*11*) and with POPC/POPG (70/30) and pure POPG SUVs at elevated peptide to lipid ratios (*54*). Clearly, the peptide conformation is highly dependent on the experimental conditions and lipid systems used.

Since, in the current study, the values of the partition constant for the various lipid compositions were found to be almost the same, the influence of the content of acidic lipids on the conformation of penetratin bound to DOPC/DOPG LUVs was examined. Figure 4 shows the circular dichroism spectra of penetratin bound to liposomes with DOPC/DOPG molar ratios of 60/40 and 80/20. Spectra were also recorded on a sample with penetratin bound to pure DOPG liposomes (data not shown). All these spectra, recorded at peptide to lipid molar ratios where no vesicle aggregation occurs, were found to be virtually superimposable, indicating that the conformation of membrane-bound penetratin is independent of the surface charge density. When evaluating the secondary structure (see Materials and Methods) from the spectra in Figure 4, the helical content was found to be 60% and no β-sheet component was detected. The fact that the peptide conformation is independent of the DOPC/DOPG ratio is in accordance with the finding that all of the binding isotherms are well described by a single K_p (see above). The formation of a defined secondary structure has been demonstrated not to be critical for the membrane translocation ability of the peptide (*4*) but should nevertheless play an important part in its membrane association.

Role of Peptide−Lipid Interactions in the Translocation Mechanism. While the mechanism of translocation as a whole is yet unknown, important clues may be found in studies of peptide−lipid interactions in model systems. Whatever steps are involved in the translocation process, the association of the peptide with the membrane must be the first stage. A study that is interesting in this context was presented by Drin et al. (*10*). Their results suggest a strong correlation between the cell association of various penetratin analogues and their cellular uptake. In the present work, we present binding isotherms that demonstrate that the affinity of penetratin for lipid membranes is largely governed by nonspecific electrostatic interactions. Also, the finding that a single partition constant describes well the experimental data, irrespective of anionic/zwitterionic lipid ratio, indicates that penetratin does not bind specifically to any of the lipids used. It is thus conceivable that, upon cell association and internalization, penetratin is enriched in domains in the heterogeneous membrane where acidic lipids are abundant, but it does not require specific lipid interactions for its membrane translocation.

Importantly, there are no indications of binding cooperativity in the experimental binding isotherms, and an excellent fit to a two-state model comprising free monomer and bound monomer is obtained. Taken together with the fact that only one spectral component for the bound state could be detected in the singular value decomposition analysis, this indicates that there are no significant amounts of oligomeric peptide species present under the experimental conditions used here. Taking into account the results of the circular dichroism measurements, our conclusion is therefore that, at low to moderate surface concentrations of peptide, penetratin is present as a monomeric α-helical species. In a previous study, we showed that penetratin does not induce pore formation in vesicles prepared from a soybean lipid mixture (*6*). We have extended that study to include a range of lipid compositions, both with natural lipids and with synthetic lipids such as those used in the present binding studies, to test for penetratin-induced leakage of vesicle-entrapped carboxyfluorescein. For no lipid composition did penetratin trigger the release of dye molecules from the liposomes (data not shown). Lack of leakage was also observed by Drin et al. (*9*) in POPC/POPG liposomes. The absence of pore formation is in agreement with membrane-associated penetratin existing as a monomeric α-helix. All in all, there are strong indications that penetratin does not translocate across lipid membranes by pore formation, as is the case for, e.g., melittin (*55*).

CONCLUSIONS

This paper presents a novel approach for quantification of the binding of a peptide to lipid membranes from fluorescence or other spectroscopic data, including an experimental procedure to prevent the adsorption of cationic

peptides to silica surfaces such as cuvette walls. This method allows construction of accurate binding isotherms and has been successfully applied to the study of the membrane-translocating peptide penetratin. The analysis of spectral data and binding isotherms with respect to the membranes of lipid vesicles of DOPC and DOPG with different surface charge densities unequivocally shows that the binding can be described in terms of a two-state model comprising one free and one membrane-bound peptide species and indicates that no significant amounts of peptide oligomers are formed in the membrane at moderate concentrations. Furthermore, the experimentally determined binding free energy can be accurately described by one electrostatic component, accounted for by a Gouy−Chapman-based model, and one hydrophobic contribution, the latter being effectively independent of the electrostatics and the DOPC/DOPG ratio. In accordance with this, we also found that the peptide conformation is the same (60% α-helix and 40% random coil), irrespective of the lipid composition.

ACKNOWLEDGMENT

We are deeply indebted to Professor Krister Holmberg for useful ideas regarding peptide adsorption to surfaces. Dr. Gunnar T. Dolphin is acknowledged for helping us with the peptide synthesis and Dr. Gunnar Stenhagen for help with the mass spectrometry experiments. Mr. Tore Eriksson is acknowledged for construction of technical equipment.

REFERENCES

1. Lindgren, M., Hällbrink, M., Prochiantz, A., and Langel, Ü. (2000) *Trends Pharmacol. Sci. 21*, 99−103.
2. Schwarze, S. R., and Dowdy, S. F. (2000) *Trends Pharmacol. Sci. 21*, 45−48.
3. Derossi, D., Joliot, A. H., Chassaing, G., and Prochiantz, A. (1994) *J. Biol. Chem. 269*, 10444−10450.
4. Derossi, D., Calvet, S., Trembleau, A., Brunissen, A., Chassaing, G., and Prochiantz, A. (1996) *J. Biol. Chem. 271*, 18188−18193.
5. Fischer, P. M., Zhelev, N. Z., Wang, S., Melville, J. E., Fåhraeus, R., and Lane, D. P. (2000) *J. Pept. Res. 55*, 163−172.
6. Thoren, P. E. G., Persson, D., Karlsson, M., and Norden, B. (2000) *FEBS Lett. 482*, 265−268.
7. Persson, D., Thoren, P. E. G., and Norden, B. (2001) *FEBS Lett. 505*, 307−312.
8. Magzoub, M., Kirk, K., Eriksson, L. E. G., Langel, U., and Gräslund, A. (2001) *Biochim. Biophys. Acta 1512*, 77−89.
9. Drin, G., Demene, H., Temsamani, J., and Brasseur, R. (2001) *Biochemistry 40*, 1824−1834.
10. Drin, G., Mazel, M., Clair, P., Mathieu, D., Kaczorek, M., and Temsamani, J. (2001) *Eur. J. Biochem. 268*, 1304−1314.
11. Bellet-Amalric, E., Blaudez, D., Desbat, B., Graner, F., Gauthier, F., and Renault, A. (2000) *Biochim. Biophys. Acta 1467*, 131−143.
12. Fragneto, G., Graner, F., Charitat, T., Dubos, P., and Bellet-Amalric, E. (2000) *Langmuir 16*, 4581−4588.
13. Berlose, J. P., Convert, O., Derossi, D., Brunissen, A., and Chassaing, G. (1996) *Eur. J. Biochem. 242*, 372−386.
14. Lindberg, M., and Gräslund, A. (2001) *FEBS Lett. 497*, 39−44.
15. Schwarz, G., and Beschiaschvili, G. (1989) *Biochim. Biophys. Acta 979*, 82−90.
16. Beschiaschvili, G., and Seelig, J. (1990) *Biochemistry 29*, 52−58.
17. Dathe, M., Schumann, M., Wieprecht, T., Winkler, A., Beyermann, M., Krause, E., Matsuzaki, K., Murase, O., and Bienert, M. (1996) *Biochemistry 35*, 12612−12622.
18. Turner, D. C., Straume, M., Kasimova, M. R., and Gaber, B. P. (1995) *Biochemistry 34*, 9517−9525.
19. Wieprecht, T., Apostolov, O., Beyermann, M., and Seelig, J. (1999) *J. Mol. Biol. 294*, 785−794.
20. Breukink, E., Ganz, P., de Kruijff, B., and Seelig, J. (2000) *Biochemistry 39*, 10247−10254.
21. Beschiaschvili, G., and Seelig, J. (1990) *Biochemistry 29*, 10995−11000.
22. Seelig, A., Alt, T., Lotz, S., and Holzemann, G. (1996) *Biochemistry 35*, 4365−4374.
23. Schwarz, G., Gerke, H., Rizzo, V., and Stankowski, S. (1987) *Biophys. J. 52*, 685−692.
24. Hellmann, N., and Schwarz, G. (1998) *Biochim. Biophys. Acta 1369*, 267−277.
25. Frey, S., and Tamm, L. K. (1990) *Biochem. J. 272*, 713−719.
26. Pouny, Y., Rapaport, D., Mor, A., Nicolas, P., and Shai, Y. (1992) *Biochemistry 31*, 12416−12423.
27. McLaughlin, S. (1989) *Annu. Rev. Biophys. Biophys. Chem. 18*, 113−136.
28. Mayer, L. D., Hope, M. J., and Cullis, P. R. (1986) *Biochim. Biophys. Acta 858*, 161−168.
29. New, R. R. C. (1990) in *Liposomes—a practical approach* (New, R. R. C., Ed.) pp 108−109, IRL Press/Oxford University Press, Oxford.
30. Perczel, A., Park, K., and Fasman, G. D. (1992) *Anal. Biochem. 203*, 83−93.
31. Grant, E., Jr., Beeler, T. J., Taylor, K. M., Gable, K., and Roseman, M. A. (1992) *Biochemistry 31*, 9912−9918.
32. Tosteson, M. T., Holmes, S. J., Razin, M., and Tosteson, D. C. (1985) *J. Membr. Biol. 87*, 35−44.
33. Duncan, M. R., Lee, J. M., and Warchol, M. P. (1995) *Int. J. Pharmacol. 120*, 179−188.
34. Brink, C., Österberg, E., Holmberg, K., and Tiberg, F. (1992) *Colloids Surf. 66*, 149−156.
35. Stankowski, S., Wey, J., Kalb, E., and Goundis, D. (1991) *Biochim. Biophys. Acta 1068*, 61−67.
36. Mishra, V. K., and Palgunachari, M. N. (1996) *Biochemistry 35*, 11210−11220.
37. Schmitz, A. A. P., Ulrich, A., and Vergeres, G. (2000) *Arch. Biochem. Biophys. 380*, 380−386.
38. Ladokhin, A. S., Jayasinghe, S., and White, S. H. (2000) *Anal. Biochem. 285*, 235−245.
39. Matsuzaki, K., Murase, O., Tokuda, H., Funakoshi, S., Fujii, N., and Miyajima, K. (1994) *Biochemistry 33*, 3342−3349.
40. Schwarz, G. (2000) *Biophys. Chem. 86*, 119−129.
41. Polozov, I. V., Polozova, A. I., Mishra, V. K., Anantharamaiah, G. M., Segrest, J. P., and Epand, R. M. (1998) *Biochim. Biophys. Acta 1368*, 343−354.
42. Lawson, C. L., and Hanson, R. J. (1974) *Solving Least Squares Problems*, Prentice-Hall, New Jersey.
43. Seelig, J., Nebel, S., Ganz, P., and Bruns, C. (1993) *Biochemistry 32*, 9714−9721.
44. Eisenberg, M., Gresalfi, T., Riccio, T., and McLaughlin, S. (1979) *Biochemistry 18*, 5213−5223.
45. Stankowski, S. (1991) *Biophys. J. 60*, 341−351.
46. Carnie, S., and McLaughlin, S. (1983) *Biophys. J. 44*, 325−332.
47. Seelig, A., and Macdonald, P. M. (1989) *Biochemistry 28*, 2490−2496.
48. Cantor, C. R., and Schimmel, P. R. (1980) *Biophysical Chemistry*, Vol. 1, W. H. Freeman, San Fransisco.
49. White, S. H., and Wimley, W. C. (1998) *Biochim. Biophys. Acta 1376*, 339−352.
50. Ladokhin, A. S., and White, S. H. (1999) *J. Mol. Biol. 285*, 1363−1369.
51. Wimley, W. C., and White, S. H. (1996) *Nat. Struct. Biol. 3*, 842−848.
52. Hristova, K., and White, S. H. (2000) *Biophys. J. 78*, 78Plat.
53. Ladokhin, A. S., and White, S. H. (2001) *J. Mol. Biol. 309*, 543−552.
54. Magzoub, M., Eriksson, L. E. G., and Gräslund, A. (2002) *Biochim. Biophys. Acta 1563*, 53−63.
55. Matsuzaki, K., Yoneyama, S., and Miyajima, K. (1997) *Biophys. J. 73*, 831−838.

BI026453T